ELSEVIER

Thermochimica Acta 320 (1998) 75–88

thermochimica acta

Isothermal kinetic analysis of the thermal decomposition of magnesium hydroxide using thermogravimetric data

I. Halikia*, P. Neou-Syngouna, D. Kolitsa

National Technical University of Athens (NTUA), Department of Mining and Metallurgical Engineering, Section of Metallurgy and Materials Technology, Laboratory of Metallurgy, 9 Heroon Polytechniou Str., Zografou Campus, 15780 Athens, Greece

Received 24 July 1997; accepted 1 June 1998

Abstract

In the present study, the kinetics of the thermal decomposition of magnesium hydroxide is investigated, using isothermal methods of kinetic analysis. For this purpose, experiments in thermogravimetric analyser were carried out in standard values of temperature (350°, 400°, 450° and 500°C) which resulted in weight loss percent as a function of time. The data were further modified to give fraction reacted 'α' versus time to be tested in various forms of 'α' functions. In order to determine the mechanism of the magnesium hydroxide decomposition and the form of the conversion function which governs the dehydroxylation of $Mg(OH)_2$, four different methods of isothermal kinetic analysis were used. Applying each of these methods to the data, it was concluded that the nucleation mechanism predominates the $Mg(OH)_2$, decomposition for all values of temperature tested; at 350°C the kinetic model which represents the experimental data is that of reaction at phase boundaries (random nucleation), F_1: $\ln(1-\alpha)=kt$) while for the higher temperatures 400°, 450° and 500°C the kinetic equation of nucleation and development in two dimensions, A_2: $[-\ln(1-\alpha)]^{1/2}=kt$ was found to fit better the experimental results. The activation energy was evaluated applying two alternative methods; the Arrhenius plot, using maximum rates of reaction, from which the activation energy was evaluated to be 20.54 kcal/mol. An alternative method based on plots of $\ln t$ versus $1/T$ corresponding to the same value of 'α' gave values of 10.72, 13.82 and 16.31 kcal/mol for 'α' values of 0.25, 0.50 and 0.75, respectively. © 1998 Elsevier Science B.V.

1. Introduction

The kinetics of many solid-state reactions can be represented by the general equation

$$f(\alpha) = kt, \tag{1}$$

where α is the fraction reacted in time t and the function $f(\alpha)$ depends on the reaction mechanism and the geometry of the reacting particles.

Two alternative methods have been used in kinetic investigations of thermal decomposition and, indeed, other reactions of solids [1,2]: In one, yield-time measurements are made while the reactant is maintained at a constant (known) temperature (isothermal method) while, in the second, the sample is subjected to a controlled rising temperature (nonisothermal method).

Measurements using both techniques have been widely and variously exploited in the determination of kinetic characteristics and parameters.

The rate-determining step in any solid-phase reaction [3] can be either (i) diffusion, i.e the transportation of participants to, or from, a zone of preferred reaction, or (ii) a chemical reaction, i.e. one or more bond redistribution steps, generally occurring at a

*Corresponding author. Tel.: 0030 1 7722188; fax: 00301 1 7722218.

0040-6031/98/$19.00 © 1998 Elsevier Science B.V. All rights reserved
PII S0040-6031(98)00413-4

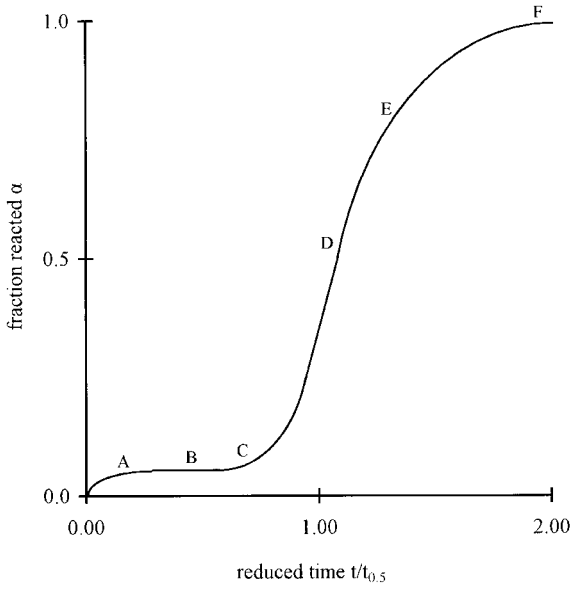

Fig. 1. Generalized α-time plot summarizing characteristic kinetic behaviour observed for isothermal decomposition of solids. There are wide variations in the relative significance of the various stages (distinguished by letters in the diagram). Some stages may be negligible or absent, many reactions of solids are deceleratory throughout. A, initial reaction (often deceleratory); B, induction period; C, acceleratory period; D, point of inflection at maximum rate (in some reactions there is an appreciable period of constant rate); E, deceleratory (or decay) period; and F, completion of reaction.

reaction interface. Intermediate behaviour, and transition regions from one type to the other, are also known. These two fundamental processes are based on the assumption that, initially, surface diffusion rapidly coats the surface of the reacting particle with a continuous product layer. There is, however, another way of looking at the initial product formation and subsequent growth. This approach considers the nucleation of products at active sites and the rate at which the nucleated particles grow [3,4].

According to this state, the known kinetic functions $f(\alpha)$ have been classified into three groups: the diffusion, the chemical reaction, and the nucleation model. Features of α-time curves for reactions of solids are of characteristic sigmoid shape, as can be seen from Fig. 1 [3], a generalized reduced-time plot in which time values have been scaled to $t_{0.5}=1.00$ when $\alpha=0.5$. A is an initial reaction, sometimes associated with the decomposition of impurities or unstable superficial material. B is the induction period, usually regarded as being terminated by the development of stable nuclei (often completed at a low value of α. C is the acceleratory period of growth of such nuclei, perhaps accompanied by further nucleation, and which extends to the maximum rate of reaction at D. Thereafter, the continued expansion of nuclei is no longer possible, due to impingement and consumption of reactant and this leads to the deceleratory or decay period, E, which continues until completion of reaction, F. One or more of these stages (except D) may be absent or negligible; variations in their relative importance results in the appearance of a wide variety of different types of kinetic behaviour.

In isothermal techniques many methods of kinetic analysis have been used for determining the reaction mechanism, i.e. the kinetic model $f(\alpha)$. In this paper, the most commonly methods for isothermal kinetic analysis are used in order to determine the mechanism of $Mg(OH)_2$ decomposition using thermogravimetric analyser, and evaluate the activation energy.

2. Literature review

Sinel'nikov and Gropyanov [5], regard the $Mg(OH)_2$ thermal decomposition as a reaction proceeding in four individual stages and using the non-isothermal thermogravimetric method, determined the kinetic parameters and kinetic equations of each one. The four stages they studied are:

At 20–300°C, the release of molecular water which is represented by the first-order equation $f(\alpha)=kt$, $E\alpha_3=9.78$ kcal/mol.

At 300–400°C, the breaking of Mg–OH bonds, $E\alpha_2=47.85$ kcal/mol.

At 400–600°C, the formation of intermediate dehydration products, $E\alpha_1=14.35$ kcal/mol.

For the second and the third stage obey the equation:

$$f(\alpha) = \left[\left(\frac{1}{1-\alpha}\right)^{1/3} - 1\right]$$

At 600–1000°C, the decomposition of intermediate structures represents the mechanism of

random nuclei production of the new phase, $E\alpha_4$= 35.05 kcal/mol.

Griva and Rosenband [6], using the nonisothermal thermogravimetric method for the 300–400°C range , found a value of 20.54 kcal/mol for the activation energy of the $Mg(OH)_2$ thermal decomposition.

Bhatti, Dollimore and Dyer [7] using the differential thermal analysis, found the equation

$$\left[\frac{1}{(1-\alpha)^{1/3}} - 1\right]^2 = kt$$

to be representative of the kinetics of $Mg(OH)_2$ thermal decomposition, with a determined mean value of activation energy of 49 kcal/mol.

Yoshioko, Amita and Hashozume [8] studied the thermal decomposition of $Mg(OH)_2$ with the isothermal method, and suggested that the model of nuclei production and development of the interface in two directions should successfully describe its kinetics.

The dehydroxylation of brucite was also studied by other investigators proposing a phase-boundary controlled mechanism in two dimensions [9], in three dimensions [10–12] and in a mechanism which follows first-order kinetics [12].

3. Experimental procedure

A Perkin–Elmer, TG_2, thermogravimetric analyser was used to carry out the isothermal $Mg(OH)_2$ decomposition experiments. The $Mg(OH)_2$ material used was of high purity grade, artificially produced in laboratory, abroad. The temperatures of 350°, 400°, 450° and 500°C were selected for the tests, with initial sample weight of 19.9864, 19.9445, 20.1396 and 22.5468 mg, respectively. The applying atmosphere was nitrogen.

4. Results

$Mg(OH)_2$ decomposes to MgO and H_2O according to the following reaction

$$Mg(OH)_2 \rightarrow MgO + H_2O \quad (2)$$

The plots of percent weight loss versus time, produced by the analyser for the temperatures examined are presented in Figs. 2–5, and served as the basis, for the calculation of the fraction reacted (α) in time t, according to the relationship

$$\alpha = m_t/m_0$$

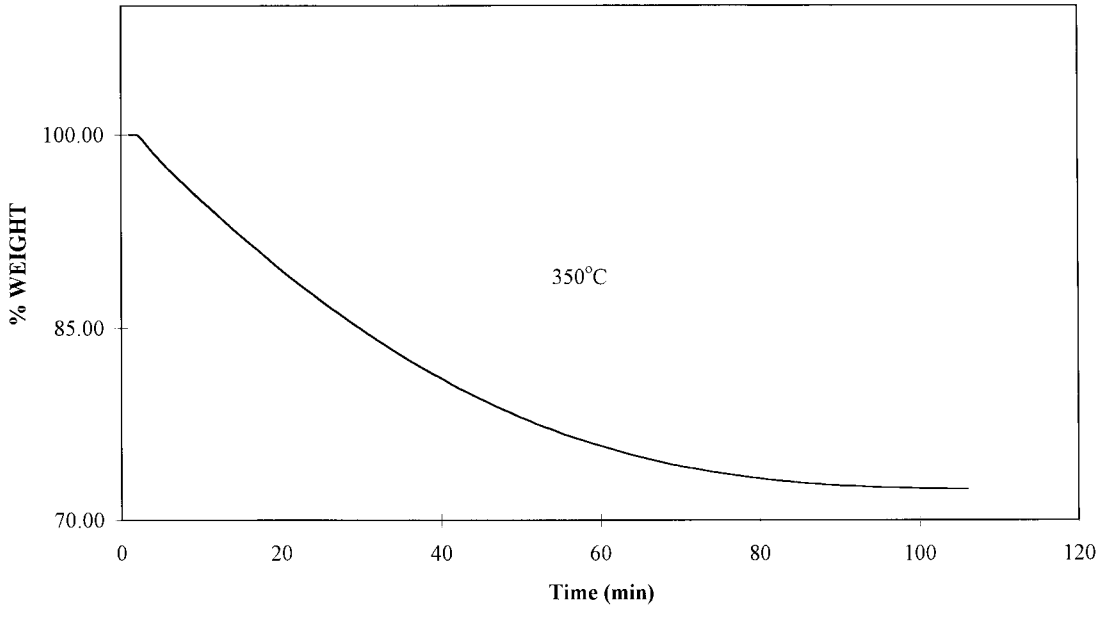

Fig. 2. Weight loss versus time for the thermal decomposition of $Mg(OH)_2$ at T=350°C.

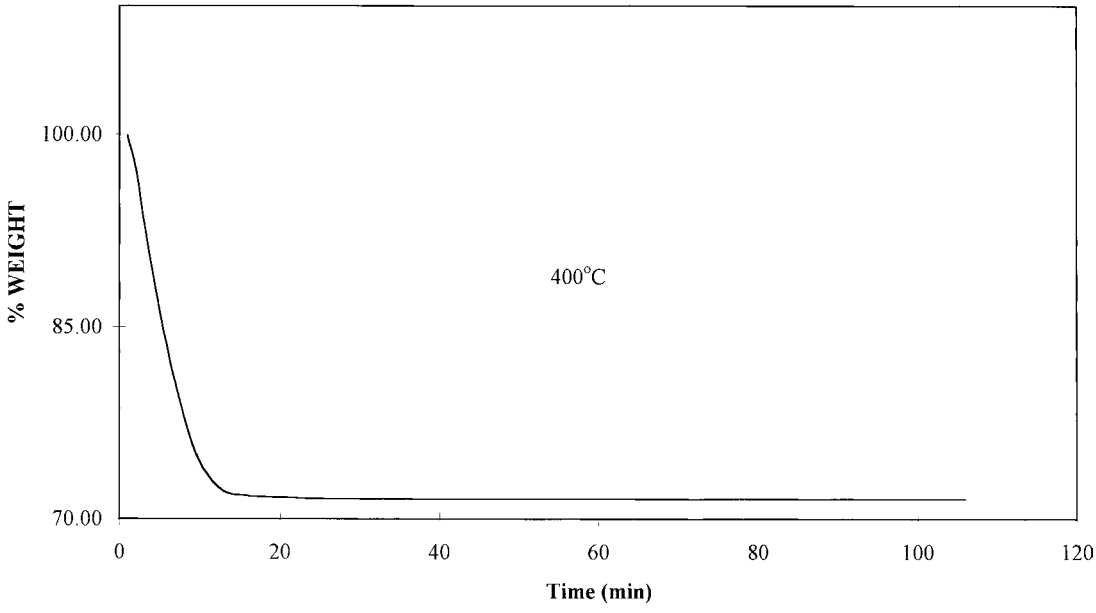

Fig. 3. Weight loss versus time for the thermal decomposition of $Mg(OH)_2$ at T=400°C.

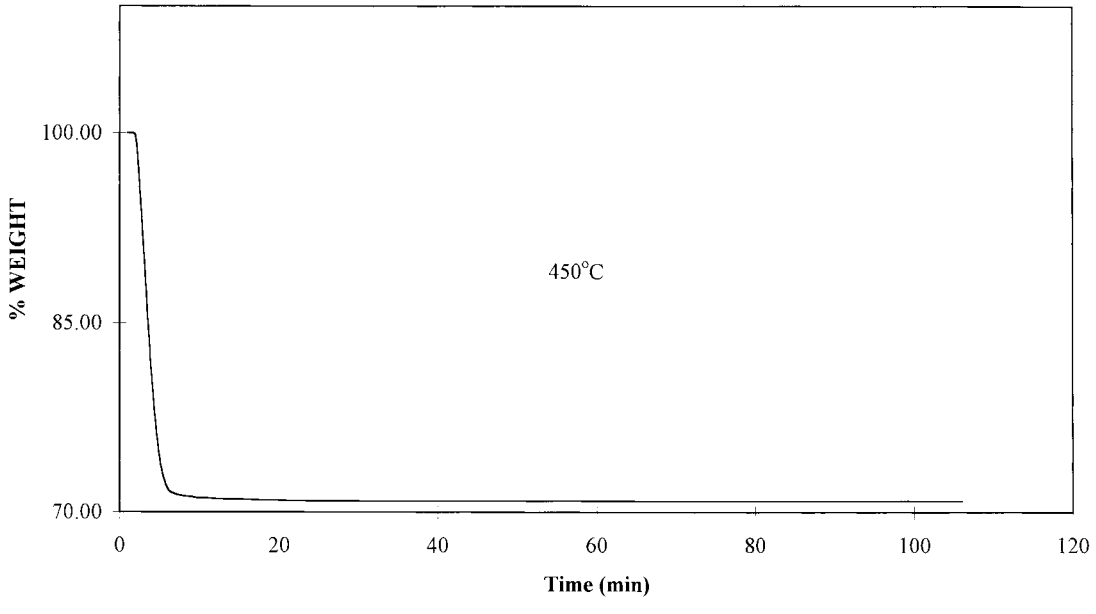

Fig. 4. Weight loss versus time for the thermal decomposition of $Mg(OH)_2$ at T=450°C.

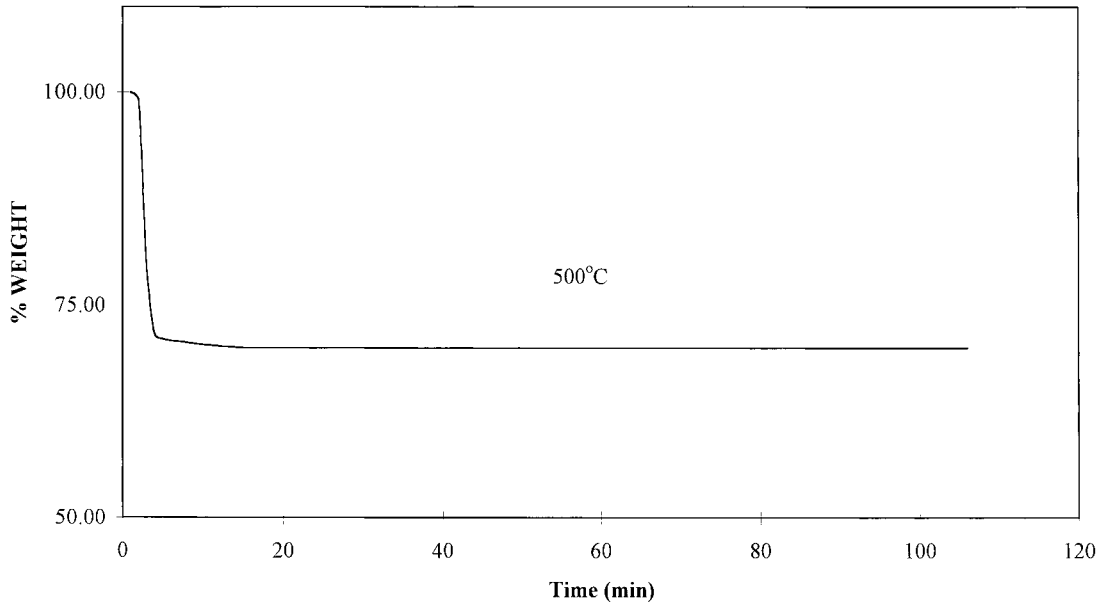

Fig. 5. Weight loss versus time for the thermal decomposition of $Mg(OH)_2$ at T=500°C.

where m_t is the percent weight loss in time t and m_0 the theoretical total weight loss (30.01%). The fraction reacted α versus time for the various temperatures is graphically presented in Figs. 6–9.

The rate of reaction ($d\alpha/dt$), given by the relationship

$$d\alpha/dt = \frac{m_t/\min}{m_0}$$

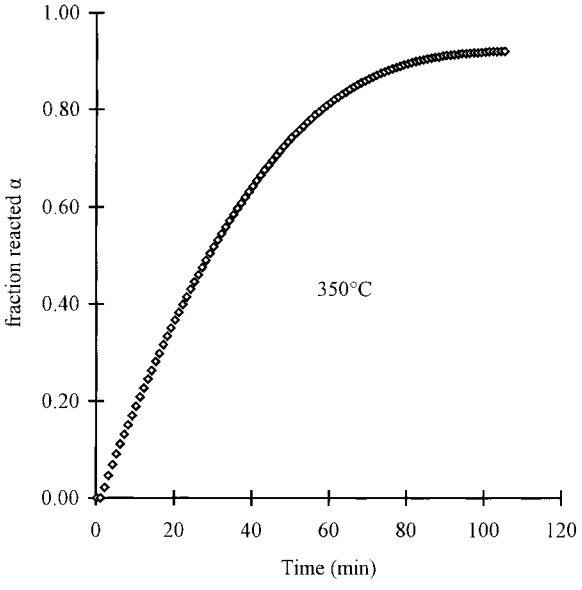

Fig. 6. Fraction reacted (α) versus time for the thermal decomposition of $Mg(OH)_2$ at T=350°C.

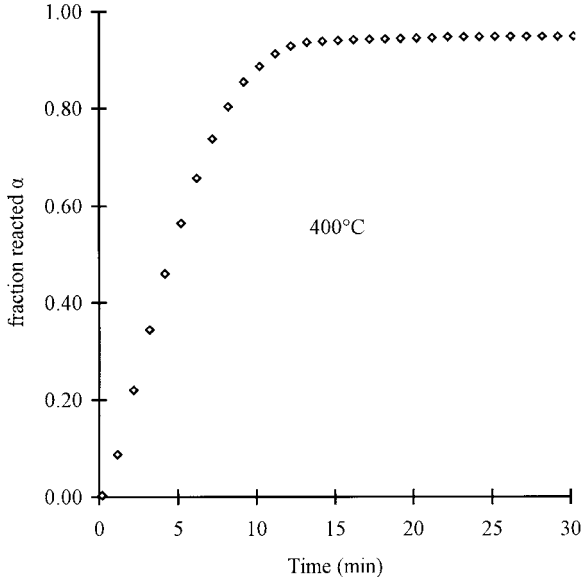

Fig. 7. Fraction reacted (α) versus time for the thermal decomposition of $Mg(OH)_2$ at T=400°C.

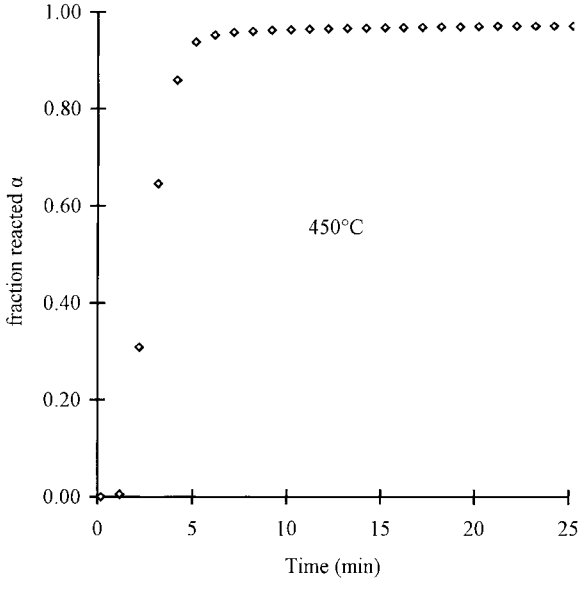

Fig. 8. Fraction reacted (α) versus time for the thermal decomposition of $Mg(OH)_2$ at T=450°C.

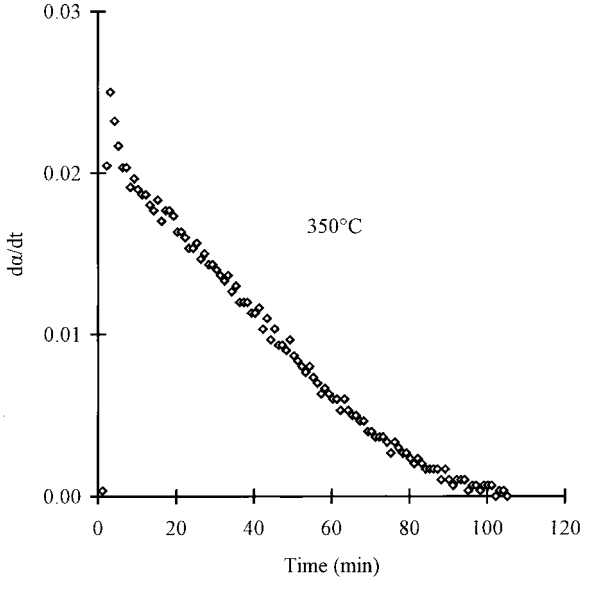

Fig. 10. Rate of reaction ($d\alpha/dt$) versus time for the thermal decomposition of $Mg(OH)_2$ at T=350°C.

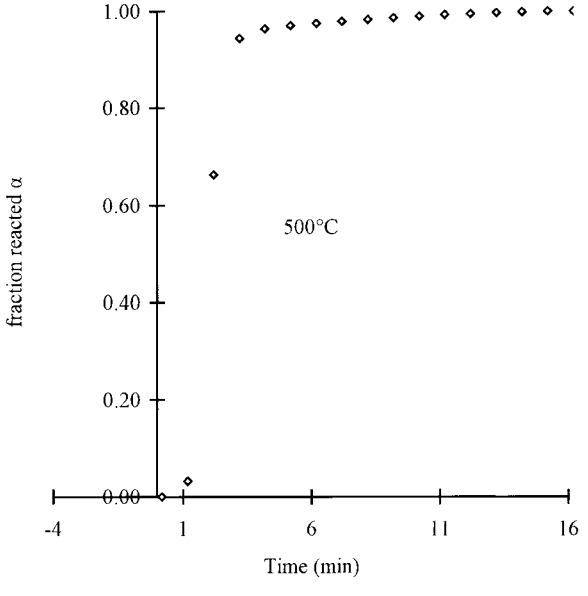

Fig. 9. Fraction reacted (α) versus time for the thermal decomposition of $Mg(OH)_2$ at T=500°C.

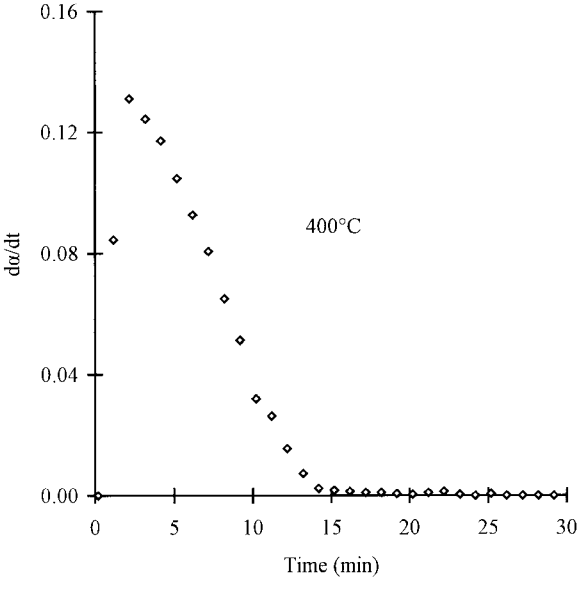

Fig. 11. Rate of reaction ($d\alpha/dt$) versus time for the thermal decomposition of $Mg(OH)_2$ at T=400°C.

was determined and its values are graphically represented as function of time in Figs. 10–13. These experimental data were further kinetically treated and analysed in order to determine the controlling mechanism and the underlying equations.

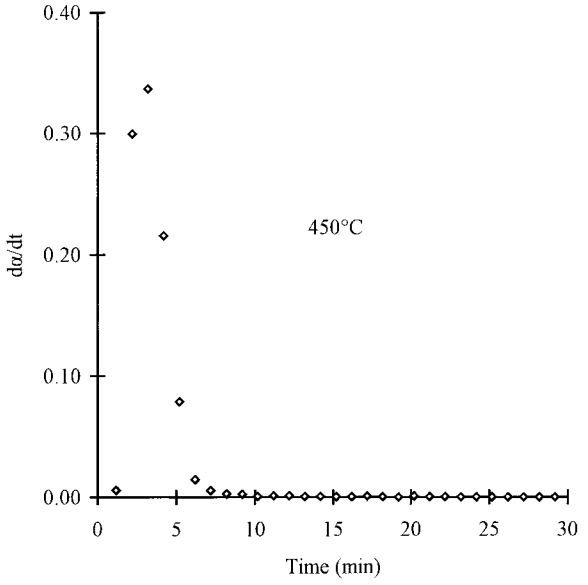

Fig. 12. Rate of reaction ($d\alpha/dt$) versus time for the thermal decomposition of $Mg(OH)_2$ at T=450°C.

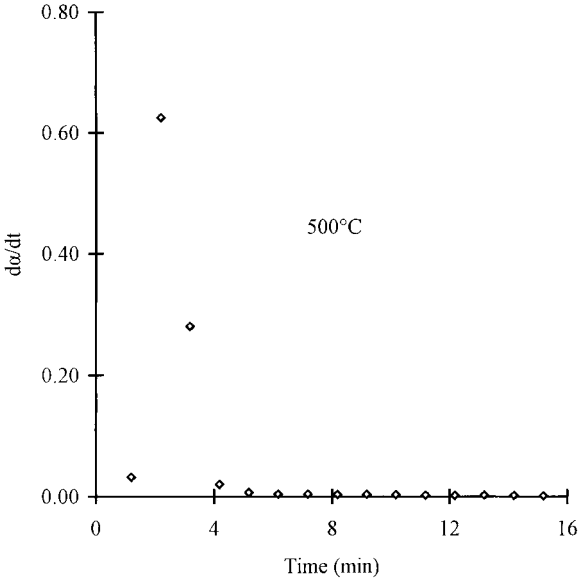

Fig. 13. Rate of reaction ($d\alpha/dt$) versus time for the thermal decomposition of $Mg(OH)_2$ at T=500°C.

5. Kinetic analysis

For the kinetic analysis of the experimentally obtained and further calculated data, the following methods were used:

First method: This method consists in comparing the experimental data – in the form of reduced time $t/t_{0.5}$ – with well-known calculated data for the most commonly used solid-state reaction equations (Table 1), as presented in Table 2 [13]. Actually, the aim was to rule out reaction-controlling mechanisms rather than discovering the exact underlying ones, since for each separate group of equations the values of $t/t_{0.5}$ are too similar to each other.

As can be seen from Tables 3–6, equations R_2 and R_3 best fit the experimental results for 350°C, the first one for $\alpha \leq 0.7$, whereas the second for $\alpha \geq 0.7$. Equation A_2 seems to be the most suitable for tests carried out at temperatures 400° and 450°C, at 400°C for $\alpha \leq 0.7$, whereas at 450°C for $0.1 \leq \alpha \leq 0.9$ Figs. 14–17.

A definite observation is the change of the reaction mechanism from 350° to 400°C which was further reinforced by the fact that the percent weight loss versus time curve at 350°C has not the same shape as the corresponding curves for the higher temperatures.

Table 1
Values of 'n' for the most commonly used solid-state reaction equations

Kinetic equation	Values of 'n'
D_1: $\alpha^2=kt$	0.62
D_2: $(1-\alpha)\ln(1-\alpha)+\alpha=kt$	0.57
D_3: $[1-(1-\alpha)^{1/3}]^2=kt$	0.54
D_4: $1-\left(\frac{2}{3}\right)\alpha-(1-\alpha)^{2/3}=kt$	0.57
F_1: $-\ln(1-\alpha)=kt$	1.00
R_2: $1-(1-\alpha)^{1/2}=kt$	1.11
R_3: $1-(1-\alpha)^{1/3}=kt$	1.07
Zero order: $\alpha=kt$	1.24
A_2: $[-\ln(1-\alpha)]^{1/2}=kt$	2.00
A_3: $[-\ln(1-\alpha)]^{1/3}=kt$	3.00
Prout: $-\ln(\alpha/1-\alpha)=kt$ (1)	
−Tompkins: $\ln(\alpha/1-\alpha)=k\ln t$ (2)	

Second method: From the widely applied equation

$$\ln[-\ln(1-\alpha)] = n\ln t + \ln k],$$

characteristic values of 'n', which represents the slope of the lines produced, have been established for the most commonly used solid-state reaction equations and are represented in Table 1[14]. For values of the experimentally calculated fraction reacted (α) ranging

Table 2
Values of α and $t/t_{0.5}$ for the most commonly used solid-state reaction equations

α	$D_1(\alpha)$	$D_2(\alpha)$	$D_3(\alpha)$	$D_4(\alpha)$	$F_1(\alpha)$	$R_2(\alpha)$	$R_3(\alpha)$	$A_2(\alpha)$	$A_3(\alpha)$
0.1	0.040	0.033	0.028	0.032	0.152	0.174	0.165	0.390	0.533
0.2	0.160	0.140	0.121	0.135	0.322	0.362	0.349	0.567	0.685
0.3	0.360	0.328	0.395	0.324	0.515	0.556	0.544	0.717	0.801
0.4	0.640	0.609	0.576	0.595	0.737	0.768	0.762	0.858	0.903
0.5	1.000	1.000	1.000	1.000	1.000	1.000	1.000	1.000	1.000
0.6	1.440	1.521	1.628	1.541	1.332	1.253	1.277	1.150	1.097
0.7	1.960	2.207	2.568	2.297	1.737	1.543	1.607	1.318	1.198
0.8	2.560	3.115	4.051	3.378	2.322	1.887	2.014	1.524	1.322
0.9	3.240	4.363	6.747	5.028	3.322	2.334	2.602	1.822	1.492

Table 3
Values of α versus $t/t_{0.5}$ for the thermal decomposition of $Mg(OH)_2$ at T=350°C, whereby $t_{0.5}$=28.67 min

$t/t_{0.5}$	α	$t/t_{0.5}$	α	$t/t_{0.5}$	α
0.0000	0.0000	1.2271	0.5838	2.4827	0.8667
0.0063	0.0000	1.2619	0.5958	2.5176	0.8704
0.0408	0.0003	1.2968	0.6078	2.5525	0.8740
0.0760	0.0210	1.3317	0.6198	2.5874	0.8774
0.1109	0.0460	1.3666	0.6311	2.6223	0.8800
0.1454	0.0690	1.4015	0.6425	2.6571	0.8834
0.1803	0.0906	1.4363	0.6541	2.6920	0.8864
0.2152	0.1110	1.4712	0.6644	2.7269	0.8890
0.2501	0.1313	1.5061	0.6754	2.7618	0.8917
0.2853	0.1506	1.5410	0.6851	2.7967	0.8940
0.3202	0.1703	1.5759	0.6954	2.8315	0.8960
0.3551	0.1893	1.6107	0.7048	2.8664	0.8984
0.3900	0.2079	1.6456	0.7141	2.9013	0.9004
0.4248	0.2266	1.6805	0.7231	2.9362	0.9020
0.4597	0.2446	1.7154	0.7328	2.9710	0.9037
0.4946	0.2622	1.7503	0.7414	3.0059	0.9054
0.5295	0.2806	1.7851	0.7498	3.0408	0.9070
0.5644	0.2976	1.8200	0.7577	3.0757	0.9080
0.5992	0.3152	1.8549	0.7654	3.1106	0.9097
0.6341	0.3329	1.8898	0.7734	3.1454	0.9107
0.6690	0.3502	1.9247	0.7807	3.1803	0.9114
0.7039	0.3665	1.9595	0.7877	3.2152	0.9124
0.7388	0.3829	1.9944	0.7941	3.2501	0.9134
0.7736	0.3989	2.0293	0.8007	3.2850	0.9144
0.8085	0.4142	2.0642	0.8071	3.3198	0.9147
0.8434	0.4295	2.0991	0.8131	3.3547	0.9154
0.8783	0.4452	2.1339	0.8191	3.3896	0.9160
0.9131	0.4598	2.1688	0.8244	3.4245	0.9164
0.9480	0.4748	2.2037	0.8304		0.9170
0.9829	0.4892	2.2386	0.8357	3.4942	0.9177
1.0178	0.5035	2.2735	0.8407	3.5291	0.9184
1.0527	0.5175	2.3083	0.8457	3.5640	0.9184
1.0875	0.5312	2.3432	0.8504	3.5989	0.9187
1.1224	0.5445	2.3781	0.8550	3.6338	0.9190
1.1573	0.5581	2.4130	0.8590	3.6686	0.9190
1.1922	0.5708	2.4479	0.8630		

Table 4
Values of α versus $t/t_{0.5}$ for the thermal decomposition of $Mg(OH)_2$ at T=400°C, whereby $t_{0.5}$=5.52 min

$t/t_{0.5}$	α
0.0000	0.0000
0.0326	0.0033
0.2120	0.0870
0.3949	0.2193
0.5761	0.3436
0.7554	0.4595
0.9366	0.5641
1.1178	0.6568
1.2989	0.7374
1.4819	0.8031
1.6630	0.8544
1.8442	0.8864
2.0254	0.9127
2.2065	0.9284
2.3877	0.9357
2.5688	0.9380
2.7500	0.9397
2.9312	0.9410
3.1123	0.9420
3.2935	0.9430
3.4746	0.9437
3.6558	0.9440
3.8370	0.9450
4.0181	0.9464
4.1993	0.9467
4.3804	0.9467
4.5616	0.9474
4.7428	0.9474

Table 5
Values of α versus $t/t_{0.5}$ for the thermal decomposition of $Mg(OH)_2$ at T=450°C, whereby $t_{0.5}$=2.7 min

$t/t_{0.5}$	α
0.0000	0.0000
0.0667	0.0000
0.4333	0.0057
0.8074	0.3082
1.1778	0.6448
1.5444	0.8584
1.9148	0.9374
2.2852	0.9517
2.6556	0.9570
3.0296	0.9597
3.4000	0.9620
3.7704	0.9627
4.1407	0.9640
4.5111	0.9653
4.8815	0.9660
5.2519	0.9667
5.6222	0.9670
5.9926	0.9673
6.3630	0.9683
6.7333	0.9687
7.1037	0.9687
7.4741	0.9697
7.8444	0.9700
8.2148	0.9703
8.5852	0.9703
8.9556	

from 0.15 to 0.5 the following values of 'n' have been found and the linearity of the diagrams obtained was ensured by the least-squares method:

For 350°C, 'n' had a value of 1.14, denoting that chemical reaction was the $Mg(OH)_2$ decomposition controlling mechanism, without being further able to determine the exact equation.

For 400°C, 'n' had a value of 1.87, which implies that nucleation is the controlling mechanism, equation A_2 being most likely to fit.

For the experiments in 450° and 500°C, this method cannot be applied since the reaction of thermal decomposition takes place too fast and only one value of α can be taken in the interval $0.1 \leq \alpha \leq 0.9$.

Third method: For the already mentioned equations (Table 1), the correlation coefficient R (obtained by substituting, in those the fraction reacted α) is an indication of the equation more likely to represent the decomposition process; the closer to the unit, the more suitable the equation.

The resulted values of α and the respective time t from the experiments in various temperatures were substituted in the above equations and the linearity was examined by the least-squares method.

As can be seen from Table 7, for 350°C, the best fitting for the data was observed for the equations that are typical of chemical reaction (R_2, R_3 and F_1).

For 400°C, all possible sigmoid equations (A_2, A_3 and $P-T$) exhibit correlation coefficients close to the unit; best one being that of A_2 (0.9927). Chemical reaction equations (F_1, R_2, R_3) too, provide appropriate correlation coefficients, however, it has to be mentioned that the linearization is referred only to the deceleratory part of the experimentally obtained curves.

This method was not applied for the F_1, R_2, R_3 kinetic models at the higher temperatures of 450° and

Table 6
Values of α versus $t/t_{0.5}$ for the thermal decomposition of $Mg(OH)_2$ at T=500°C, whereby $t_{0.5}$=1.89 min

$t/t_{0.5}$	α
0.0000	0.0000
0.0952	0.0000
0.6243	0.0317
1.1534	0.6631
1.6825	0.9437
2.2063	0.9637
2.7354	0.9703
3.2646	0.9747
3.7937	0.9790
4.3280	0.9827
4.8571	0.9863
5.3862	0.9893
5.9153	0.9920
6.4444	0.9940
6.9735	0.9963
7.5026	0.9980
8.0317	0.9993
8.5608	0.9993
9.0899	0.9993
9.6190	

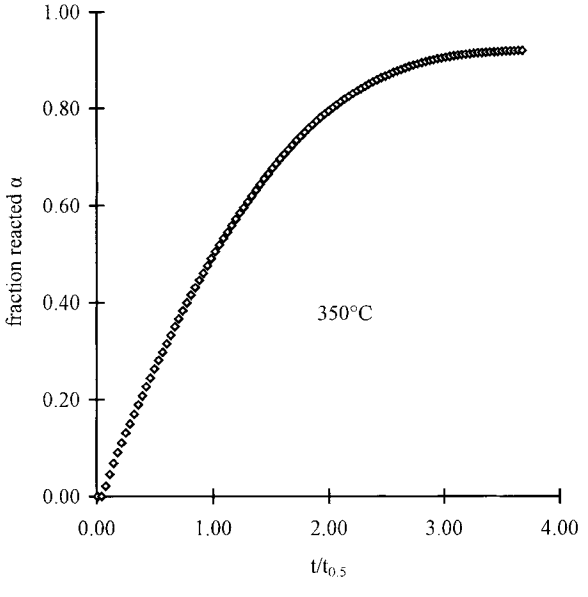

Fig. 14. Fraction reacted (α) versus $t/t_{0.5}$ for the thermal decomposition of $Mg(OH)_2$ at T=350°C, whereby $t_{0.5}$=28.67 min.

500°C, because the process was very fast and the deceleratory stage was not representative of the whole process.

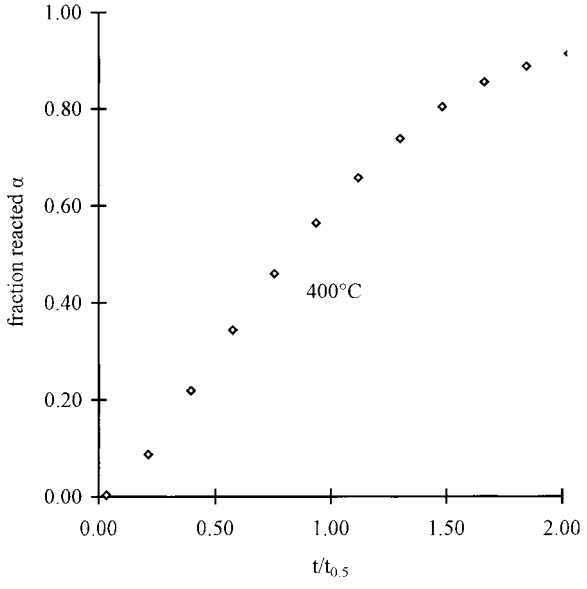

Fig. 15. Fraction reacted (α) versus $t/t_{0.5}$ for the thermal decomposition of $Mg(OH)_2$ at T=400°C, whereby $t_{0.5}$=5.52 min.

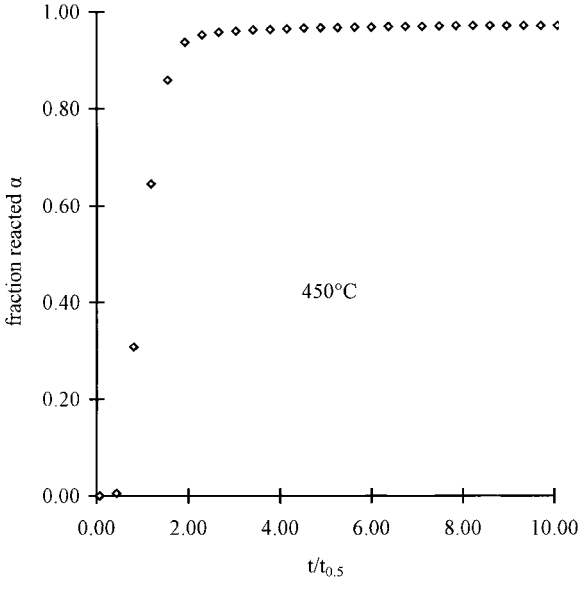

Fig. 16. Fraction reacted (α) versus $t/t_{0.5}$ for the thermal decomposition of $Mg(OH)_2$ at T=450°C, whereby $t_{0.5}$=2.7 min.

For 450°C, all sigmoid equations turned out to produce good linearity, the best one being that of A_2 (R=0.997), just as in the case of 400°C. Finally, it was not possible to establish any results for the

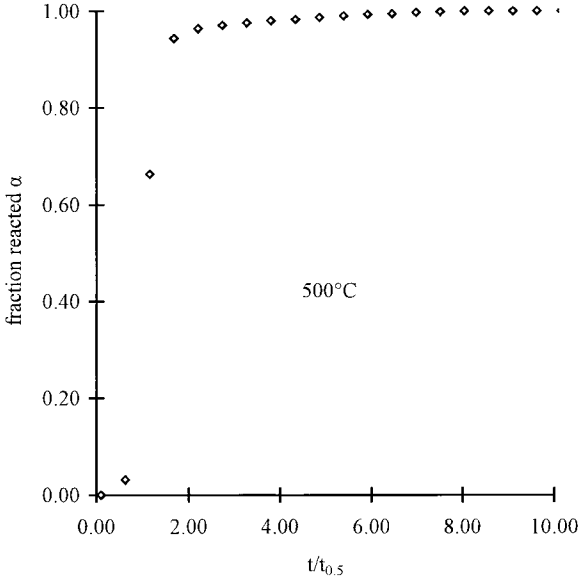

Fig. 17. Fraction reacted (α) versus $t/t_{0.5}$ for the thermal decomposition of $Mg(OH)_2$ at T=500°C, whereby $t_{0.5}$=1.89 min.

500°C experiment, by this method, because of the high rate of reaction at this temperature.

Fourth method: According to this method proposed by Tang and Chaudri [15], there are three cases in the kinetic analysis procedure, based on the differential form of the kinetic equation, depending on the value of 'n', already obtained in the preceding procedure (second method).

(a) $n \geq 2$. In this case

$$d\alpha/dt = k\alpha^p(1-\alpha)^q$$

and by the least-squares fit on the graph of $\Delta\log(d\alpha/dt)/\Delta\log\alpha$ against $\Delta\log(1-\alpha)/\Delta\log\alpha$, p and q can be calculated.

(b) $n \sim 1$. In this case

$$d\alpha/dt = k(1-\alpha)^s$$

and from the graph of $\log(d\alpha/dt)$ against $\log(1-\alpha)$, the slope s is determined.

(c) $n \sim 0.5$. In this case

$$-(d\alpha/dt)\ln(1-\alpha)^s = k(1-\alpha)^s$$

is the basic equation, with s=0 (diffusion in two dimensions) or s=1/3 (diffusion in three dimensions).

At 350°C, the value of n was found to be 1.14, which approaches that of n=1 (case b). Therefore, by plotting the diagram $\log(d\alpha/dt)$ against $\log(1-\alpha)$ (Fig. 18), for values of α between 1.1 and 1.9, the slope s of the linear portion is 0.9918, approaching the unit, meaning that the differential reaction equation is transformed as follows

$$(d\alpha/dt) = k(1-\alpha),$$

and the respective kinetic equation is F_1.

Table 7
Correlation coefficients resulted by the application of the least-squares method to the experimentally obtained data for the most commonly used solid-state reaction equations

α	F_1	R_2	R_3	$A_2(\alpha)$	$A_3(\alpha)$	$(P-T)_1$	$(P-T)_2$	
T=350°C								
76 points	0.999	0.996	0.940	−0.215	0.069	0.880	0.910	
α	F_1	R_2	R_3	$\alpha=kt$	A_2	A_3	$(P-T)_1$	$(P-T)_2$
T=400°C								
3 points				0.991				
8 points	0.997	0.999	0.999					
9 points	0.995	0.985	0.999					
10 points					0.992	0.970	0.905	0.984
11 points					0.993	0.970	0.910	0.986
12 points					0.993	0.969	0.914	0.987
α	A_2	A_3	$(P-T)_1$	$(P-T)_2$				
T=450°C								
3 points	0.997	0.987	0.960	0.989				
4 points	0.997	0.982	0.948	0.989				
5 points	0.993	0.973	0.941	0.989				

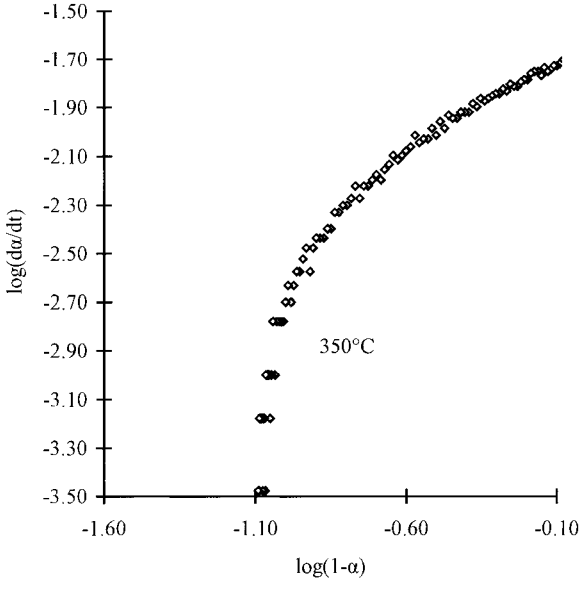

Fig. 18. Log (dα/dt) versus log (1−α) for the differential equation form: log (dα/dt)=log k+r log(1−α) at T=350°C.

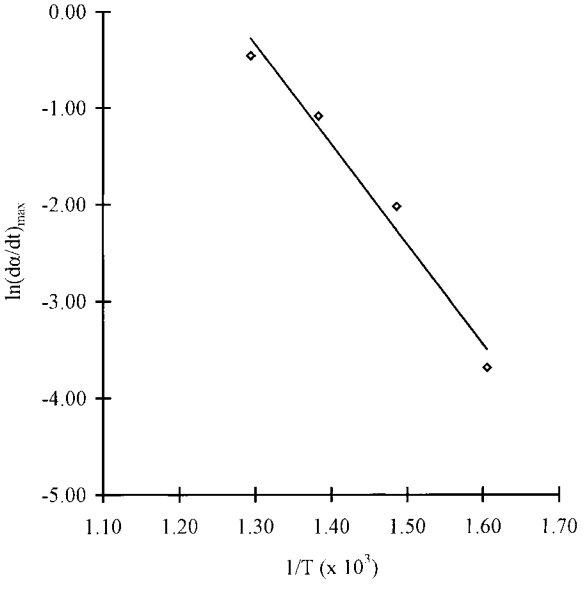

Fig. 19. Arrhenius plot with the use of maximum rates.

At 400°C, the value of n=1.87 approaches that of n=2 (case a). From the diagram plotted, unfortunately, the p and q values are not stable, therefore, no conclusion can be drawn.

This method could not be employed for the higher temperatures of 450° and 500°C, due to the high rate of the reaction.

Determination of activation energy

For activation energy determination, two alternative methods were used

1. In one method, the Arrhenius equation has been used directly; for this purpose, the maximum rates were evaluated from the dα/dt versus time diagrams for the four values of temperature. The Arrhenius plot of ln $(\mathrm{d}\alpha/\mathrm{d}t)_{\max}$ versus 1/T is shown in Fig. 19. The activation energy determined from the slope of the straight line was 20.54 kcal/mol.
2. An alternative method was used for the activation energy determination, proposed by Haynes and Young [16]. According to this method the experimental curves (α_1, t_1) and (α_2, t_2) in different temperatures T_1 and T_2 are selected, having the same shape. It can be written that

$$\mathrm{F}(\alpha_1) = t_1 \mathrm{A} \mathrm{e}^{[-\mathrm{E}/RT_1]}$$

$$\mathrm{F}(\alpha_2) = t_2 \mathrm{A} \mathrm{e}^{[-\mathrm{E}/RT_2]}$$

For points corresponding to the same α on these corves we have F(α_1)=F(α_2). So E can be calculated from plotting ln t versus 1/T. This method was applied

Table 8
Values of ln$t$ and 1/T for the determination of the activation energy with the alternative method, and the resulted values of E

W/%	α	T	t	ln t	1/T	E/(kcal/mol)
92.50	0.2499	400°C	3.42	1.2296	1.48588×10^{-3}	
72.51	0.2499	450°C	2.01	0.6981	1.38312×10^{-3}	10.72
85.01	0.4998	400°C	5.52	1.7084	1.48588×10^{-3}	
85.01	0.4998	450°C	2.70	0.9933	1.38312×10^{-3}	13.82
77.50	0.7498	400°C	8.30	2.1163	1.48588×10^{-3}	
77.50	0.7498	450°C	3.57	1.2726	1.38312×10^{-3}	16.31

to the experimentally obtained curves of 400° and 450°C, for three values of α (0.25, 0.5, 0.75), and the corresponding time t in each temperature was determined. By plotting ln t versus $1/T$ the activation energy was calculated from the slope of the lines for each value of α. The results are presented in Table 8, from which it is observed that the values of E for the three above values of α are 10.72, 13.82 and 16.31 kcal/mol, respectively.

6. Discussion

The α–t graphs resulted from the experiments of $Mg(OH)_2$ thermal decomposition are of a typical sigmoid shape, as proved by the rate of reaction curves, which consist of an initial acceleratory portion, followed by a deceleratory one in all the temperatures tested. It is well established that sigmoid curves are to be expected at any decomposition process, and furthermore, such curves represent a process-controlling mechanism of nucleus production and growth. By applying the first two methods of kinetic analysis, it was apparent that diffusion could in no case be the controlling mechanism. Besides, the activation energy values determined by both methods exclude diffusion as rate-controlling mechanism. This means that chemical reaction and nucleus production are the candidate mechanisms, and, in fact, both are applicable, depending on the temperature. An indication that there is a change of mechanism, comes from the fact that at 350°C the experimental curve had a shape different from that at the other temperatures.

The fourth method of analysis proved F_1 to be the underlying equation at 350°C. Although F_1 is a deceleratory equation, it is nevertheless acceptable since the maximum rate of reaction is achieved for a very low value (0.046), so that the acceleratory portion is negligible compared to the deceleratory one.

At 400°C, nucleus production and development in two dimensions was found to be the controlling mechanism according to the results of the first two methods, whereas by applying the third method both chemical reaction and nucleus production and growth were possible mechanisms. The good correlation coefficient of the chemical reaction equations (F_1, R_2, R_3) can be explained by the following argument: It is well known that the deceleratory portion of the sigmoid curves of the nucleus production equations is similar to the curves of the deceleratory chemical reaction equations. For instance, at the final stage of nucleation and development, a product layer will cover the surface of the reactant and the process behaviour will be similar to the one predicted by the model of contracting volume.

By comparing the various methods of kinetic analysis that were used in the present study to predict the model underlying the dehydroxylation of $Mg(OH)_2$ thermal decomposition, the following separate groups can be recognized: That, involving the determination of the linearity; such was the case in the second, third and fourth method. On the other hand, the first method consisted in comparison with master curves and data. Therefore, the first method has the drawback that the data used was derived from the reduced time curves, meaning that it was not real one. So, it seems that the remaining methods are more reliable in order to draw conclusions.

Another point that has to be stressed out, is that the first two methods made it possible to find out only the controlling mechanism and not to discriminate the exact equation. It was the fourth method that enabled us to determine which of the kinetic equations of the already predicted controlling mechanisms truly represents the $Mg(OH)_2$ decomposition process.

The observations made in the present study about the controlling mechanism are in accordance with the conclusions of other investigators [8–12], as well as a preceding work of Halikia [17] concerning kinetic analysis of $Mg(OH)_2$ decomposition by nonisothermal methods.

The present study was focused on kinetic analysis; this alone cannot be regarded as indisputable evidence of the predominance of a particular mechanism. It has to be further supplemented from other independent evidence such as microscopic observations regarding the geometry of the development of the interface.

7. Conclusions

From the kinetic investigation of the $Mg(OH)_2$ thermal decomposition, the following main conclusions can be derived:

1. At 350°C, the controlling mechanism corresponds to chemical reaction (reaction at phase boundaries) given by the F_1 kinetic equation

$$-\ln(1-\alpha) = kt, \qquad \text{(F1)}$$

which represents a system of random nucleation on a large number of small crystallites.
2. At 400°C, the controlling mechanism corresponds to nucleation and development given by the following kinetic equations:

$$[-\ln(1-\alpha)]^{1/2} = kt \qquad \text{(A2)}$$

$$[-\ln(1-\alpha)]^{1/3} = kt \qquad \text{(A3)}$$

From these two equations, A_2 seems more representative of the experimentally obtained data according to the second method of kinetic analysis.
3. At 450° and 500°C, the controlling mechanism corresponds again to nucleus production and development according to the first method of kinetic analysis. Furthermore, by the third method of kinetic analysis at 450°C, the A_2 kinetic equation, was found to characterize the decomposition process. At both these temperatures it was difficult, if not impossible, to apply the other two methods of analysis because the whole decomposition process was too fast.
4. The activation energy of the process evaluated by the Arrhenius plot was 20.54 kcal/mol excluding diffusion as rate-controlling mechanism. By applying an alternative method based on plots of $\ln t$ versus $1/T$ (corresponding to the same value of α) the resulted activation energy was 10.72, 13.82 and 16.31 kcal/mol for α values of 0.25, 0.5, and 0.75, respectively. These high values of activation energy are in agreement with the above proposed mechanisms and in accordance with those given by other investigators [5,6,17].

References

[1] T.B. Tang, M.M. Chaundri, Journal of Thermal Analysis 18 (1980) 247.
[2] A. Jerez, Thermochimica Acta 115 (1987) 175.
[3] C.H. Bamford, C.F.H. Tipper (Eds.), Comprehensive chemical kinetics, Elsevier Scientific Publishing Corporation, 1980, vol. 22, Chap. 22.
[4] W.E. Garner (Ed.), Chemistry of the solid state, Butterworths Scientific Publications, London, 1955.
[5] S.V. Sinel'nikov, V.M. Gropyanov, Journal of Applied Chemistry of USSR 55(3) (1982) 461.
[6] V.A. Griva, V.I. Rosenband, Russian Journal of Physical Chemistry 54(10) (1980) 1530.
[7] A. Bhatti, D. Dollimore, A. Dyer, Thermochimica Acta 78 (1984) 55.
[8] H. Yoshioko, K. Amita, G. Hashizume, Netsu Sokutei 11(3) (1984) 115.
[9] P.J. Anderson, R.F. Horlock, Transactions of the Faraday Society 58(478) (1962) 1993.
[10] S.J. Gregg, R.I. Razouk, Journal of Chemical Society (1949) 36.
[11] R.C. Turner, I. Hoffmann, D. Chen, Canadian Journal of Chemistry 41(2) (1963) 251.
[12] R.S. Gordon, W.D. Kingery, Journal of American Ceramic Society 50(1) (1967) 8.
[13] J.H. Sharp, G.W. Brindley, B.N. Narahari, Achar, Journal of the American Ceramic Society 49(7) (1966) 379.
[14] J.D. Hancock, J.H. Sharp, Journal of the American Ceramic Society 55(2) (1972) 74.
[15] T.B. Tang, M.M. Chaudri, Journal of Thermal Analysis 17 (1979) 359.
[16] R.M. Haynes, D.A. Young, Discussions of the Faraday Society 31 (1961) 229.
[17] I. Halikia, A. Economakou, International Journal of Chemical Kinetics 25(8) (1993) 609.